Fluid Phase Equilibria 528 (2021) 112840

Contents lists available at ScienceDirect

Fluid Phase Equilibria

journal homepage: www.elsevier.com/locate/fluid

Molecular dynamics simulations of aqueous solutions of short chain alcohols. Excess properties and the temperature of maximum density

Encarnación García Pérez[a], Diego González-Salgado[a,*], Enrique Lomba[b]

[a] Departamento de Física Aplicada, Universidad de Vigo, Campus del Agua, Edificio Manuel Martínez-Risco, E-32004 Ourense, Spain
[b] Instituto de Química Física Rocasolano, CSIC, Calle Serrano 119, E-28006 Madrid, Spain

ARTICLE INFO

Article history:
Received 22 July 2020
Revised 15 September 2020
Accepted 23 September 2020
Available online 3 October 2020

ABSTRACT

The excess enthalpy h^E and excess volume v^E of the binary systems {methanol, ethanol, 1-propanol, 2-propanol, and tert-butanol + water} over the whole composition range at 298.15 K and the temperature of maximum density, TMD, in the alcohol diluted region were studied by MD simulations at atmospheric pressure. Our model systems were defined using the flexible version of the TIP4P/2005 model of water, the OPLS-AA for alcohols, and the geometric combining rule for all the Lennard-Jones cross interactions, with the exception of those between oxygen sites of water and alcohol molecules. These latter values were fitted to reproduce the experimental excess properties of the mixtures. This new parameterization allows for an appropriate description of the excess thermodynamics of these short-chain alcohol/water systems over the whole composition range. The changes in the temperature of maximum density of water induced by the addition of small amounts of alcohol concentration are, however, not adequately reproduced by our models. In all instances we observe a pronounced decrease of the simulated TMDs when alcohol concentration increases. This is in sharp contrast with the experimental behavior, which at very high dilution displays slight increases in the TMD right before the decreasing regime sets in for higher alcohol concentrations. For similar alcohol mole fractions, the simulated decrease of the TMDs grows in parallel with the size of the alkyl group of the alcohol. A similar situation is found experimentally for concentrations higher than those that increase the TMD. These differences disappear when the TMD change is expressed in terms of the mass concentration of alcohol. This leads to very similar Despretz constants for all solutions studied in this work.

1. Introduction

Aqueous alcohol solutions are extensively used in many different applications from everyday life to science. To name but a few, it is worth mentioning their role in the efficient exfoliation of inorganic graphene analogues [1], in the synthesis of polydopamine nano-spheres [2]), as disinfectant [3], or in solar energy devices [4]. Obviously, they are at the core of the bioethanol industry [5,6]. Additionally, research on alcohol solutions has a potential impact on biological investigations. The amphiphilic character of alcohols turns them into the simplest laboratory model to analyze the behavior of more complex biological macromolecules: hydrogen bonding, hydrophobicity and non-polar interactions are all at play in alcohol solutions, and these effects are a key to understand the behavior of biomolecules in water. From a more fundamental point of view, the thermodynamic behavior of these systems exhibits a series of anomalies, closely connected with those of water [7,8], in particular at low alcohol concentrations. Thus, small amounts of alcohol in solution induce large increases in the heat capacity, or contrary to the effect of most solutes, the temperature of maximum density of water is slightly augmented for alcohol mole fractions of the order 10^{-3}. This can qualitatively be interpreted as a result of these solutes making water even more anomalous. Already back in the forties, Franks and Evans [9] suggested that these anomalies could be explained in terms of the so-called "iceberg model". According to this model, the alkyl tails of alcohols (and other hydrophobic solutes) tend to enhance the tetrahedral structure of surrounding water molecules [10]. From the experimental point of view, the full microscopic picture of water/alcohol mixtures is still far from being completely understood [11].

From all the thermodynamic anomalies of alcohol aqueous solutions it is worth stressing the very singular effect of short-chain alcohols on the temperature of maximum density (TMD) of

* Corresponding author: Dr. Diego González, Universidad de Vigo, Departamento de Física Aplicada, Pabellón Manuel Martínez-Risco, Campus de Ourense, 32004 Ourense, Ourense, Spain,
E-mail address: dgs@uvigo.es (D. González-Salgado).

https://doi.org/10.1016/j.fluid.2020.112840
0378-3812/

water. Wada and Umeda [12] have shown that the addition of small amounts of methanol, ethanol, 1-propanol, 2-propanol, and tert-butanol (TBA) raises the TMD, in contrast with the effect of other organic solutes [13] and electrolytes [14]. This increase of the TMD is only visible in a small concentration range (typically for alcohol mole fraction x less than 0.01). For higher concentrations the TMD decreases as in regular solvents, until the density anomaly disappears. As a consequence, the change in the TMD of the mixture with respect to pure water exhibits a maximum at low alcohol mole fractions, a feature that is unique to short-chain alcohols. Qualitatively, one can interpret this effect in terms of the balance between the high density and low density (tetrahedral) structures present in liquid water. The low density structure reminiscent of ice dominates right after melting. As temperature increases, H-bonds break and a more compact high density structure occurs giving rise to the presence of a maximum (TMD). Small amounts of alcohol are fully soluble (with the hydroxil group taking part in water's H-bond network), but the alkyl groups reorganize surrounding water molecules (*iceberg effect*) enhancing the tetrahedral structure in the same way as other hydrophobic solutes do [10]. This promotion of the low density water structure then increases the TMD. Nonetheless, a quantitative picture of this phenomenon in terms of intermolecular interactions is still lacking [15].

Molecular simulation [16,17] is a powerful technique to establish a correspondence between the macroscopic behavior of a system and its intermolecular interactions. In classical simulations, it is usual to describe the molecules as a set of sites whose interactions are defined through analytic functional forms, such as springs for bonded interactions, or Lennard-Jones and/or Coulombic potentials for nonbonded interactions. The model parameter values are commonly fitted to a set of target macroscopic properties of the substance to be simulated at a given temperature and pressure. Sometimes vapor-liquid equilibrium curves are also used in the fitting procedure and in some other cases *ab initio* data are used to define the effective potential parameters. In any case, the question of parameter transferability remains open, when conditions away from the fitting range are to be simulated.

Pure substance parameterizations can be straightforwardly applied to mixtures by defining the cross interactions between sites of different species using combining rules. In fact, it is also customary to use combining rules to define interactions between sites of different type even when they belong to the same molecular species. The limitations of this approach in the latter instance are in most cases subsumed by the fitting procedure in pure substances. In the case of mixtures, however, the use of combining rules is merely an educated guess, and sometimes it is completely inappropriate. The best option then is to fit the cross interactions parameters to yield a reasonable description of the mixture thermodynamics. Given the large amount of cross interaction parameters to be fitted even in the simplest binary mixtures, this approach has not been widely exploited in the literature.

A considerable body of work has addressed the study of aqueous solutions of methanol [18–31], ethanol [18,21,26,30,31–44], 1-propanol [18,21,31,45,46], 2-propanol [18,41,46–51], and tert-butanol [22,23,34,41,52–66] using molecular simulation, in most cases Molecular Dynamics (MD). A variety of molecular models have been employed, in most of the cases resorting to simple combining rules to define cross interactions. These investigations are mainly focused on structural properties (and to a lesser extent on transport and excess thermodynamics properties). Aside from our recent simulation and experimental study on the TMD for the {methanol+water} system [67], to our knowledge, no other work has focused on the anomalous effect of short-chain alcohols at high dilution on the TMD of water using molecular simulation with realistic models.

In order to investigate further the effects of the alkyl chain length and shape of short-chain alcohols on the TMD of water, we have performed an extensive simulation study of aqueous solutions of methanol, ethanol, 1-propanol, 2-propanol, and tert-butanol. Alcohols were described using flexible OPLS-AA force fields as proposed by Jorgensen [68] and water by the TIP4P/2005f model of González and Abascal [69]. A first goal of our work has been to produce a new reliable parameterization of these systems valid over the whole composition range at ambient conditions. To that aim, and in order to reduce the computational complexity of the problem, all LJ cross parameters were set to values given by the geometric combining rule, except those between the oxygen of water (O_W) and the oxygen of the alcohols (O_{OH}). These were fitted to reproduce the experimental excess enthalpy, h^E, and the excess volume, v^E, at 298.15 K and 1 bar. Then, we have tested the ability of our mixture model to describe the changes in the TMD of water induced by the addition of small amounts of these short-chain alcohols.

2. Models and simulation details

2.1. Models

Alcohols are modeled using the OPLS-AA force field proposed by Jorgensen [68] and water is described by the TIP4P/2005f proposed by González and Abascal [69]. The potential energy U in a {alcohol+water} binary mixture is the sum of three contributions: alcohol-alcohol U^A, water-water U^W, and alcohol-water U^{AW}. In what follows explicit details of these three contributions are presented.

{*Alcohol-Alcohol*}. In the OPLS-AA force field, each atom in a molecule is considered as an interaction site. The potential energy, U^A, consists of two terms, a bonded, U^A_{bonded}, and a non-bonded contribution, $U^A_{\text{nonbonded}}$. The bonded contribution comprises energy terms stemming from bond stretching, angle bending and torsional intramolecular potentials, as follows

$$U^A_{\text{bonded}} = U^A_{\text{bond}} + U^A_{\text{angle}} + U^A_{\text{torsion}} \tag{1}$$

$$U^A_{\text{bond}} = \frac{1}{2}\sum_{a,b} k_{ab}\left(r_{ab} - {r_{ab}}^0\right)^2 \tag{2}$$

$$U^A_{\text{angle}} = \frac{1}{2}\sum_{a,b,c} k_{abc}\left(\theta_{ab} - {\theta_{abc}}^0\right)^2 \tag{3}$$

$$U^A_{\text{torsion}} = \sum_{a,b,c,d}\left(\sum_{n=0}^{5} C_n(\phi_{abcd} - 180^\circ)^n\right) \tag{4}$$

where a, b, c, d, denote atoms in the molecule, k the spring constant, r the distance, θ, the bond angle, ϕ, the dihedral angle, C_n, the Ryckaert-Bellemans constants, and the superindex 0 denotes the corresponding equilibrium values. The functional form of the non-bonding term is

$$U^A_{\text{nonbonded}} = \sum_{a,b} f_{ab}\left[4\varepsilon_{ab}\left[\left(\frac{\sigma_{ab}}{r_{ab}}\right)^{12} - \left(\frac{\sigma_{ab}}{r_{ab}}\right)^{6}\right] + \frac{1}{4\pi\varepsilon_0}\frac{q_a q_b}{r_{ab}}\right], \tag{5}$$

where $f_{ab} = 1.0$ when a and b atoms belong to different molecules, $f_{ab} = 0.0$ when they belong to the same molecule but are separated by less than three bonds, and $f_{ab} = 0.5$ when the site separation is three bonds, and again $f_{ab} = 1.0$ for larger intramolecular separations. The Lennard-Jones parameters are denoted by ε and σ, partial charges by q, and ε_0 denotes the vacuum relative permitivity. The Lennard-Jones cross parameters between atoms a and b are computed in the OPLS-AA force field from the atom characteristic

Table 1
Lennard-Jones parameters of alcohol atoms.

Atom	ε_a (kJ·mol^{-1})	σ_a (nm)	q_a (e)
H_{OH}	0	0	0.418
O_{OH}	0.711280	0.312	-0.683
C [CH_3 adjacent]	0.276144	0.350	0.145
C [CH_2 adjacent]	0.276144	0.350	0.145
C [CH adjacent]	0.276144	0.350	0.205
C [C adjacent]	0.276144	0.350	0.265
H [CH_3 adjacent]	0.125520	0.250	0.040
C [CH_3]	0.276144	0.350	-0.180
C [CH_2]	0.276144	0.350	-0.120
H	0.125520	0.250	0.060

Table 2
Bond stretching parameters of alcohols.

Atom	k_{ab} (kJ·mol^{-1}·nm^{-1})	$r_{ab}{}^0$ (nm)
H_{OH} - O_{OH}	462750.4	0.09450
O_{OH} - C	267776.0	0.14100
C- C	224262.4	0.15290
C- H	284512.0	0.10900

Table 3
Angle bond parameters of alcohols.

Atom	k_{abc} (kJ·mol^{-1}.$^{\circ-1}$)	$\theta_{abc}{}^0$ ($^\circ$)
H_{OH} - O_{OH} - C	460.240	108.500
O_{OH} – C - H	292.880	109.500
O_{OH} – C- C	418.400	109.500
C – C - H	313.800	110.700
C- C- C	488.273	112.700
H – C- H	276.144	107.800

Table 4
Ryckaert-Bellemans parameters for dihedrals in alcohols.

Atom	C_0	C_1	C_2	C_3
H_{OH} - O_{OH} – C - C	-0.44350	3.83255	0.72801	-4.11705
H_{OH} - O_{OH} – C - H	0.94140	2.82420	0.00000	-3.76560
O_{OH} – C – C - H	0.97905	2.93716	0.00000	-3.91622
O_{OH} – C – C - C	2.87441	0.58158	2.09200	-5.54799
C – C - C - H	0.62760	1.88280	0.00000	-2.51040
H – C – C - H	0.62760	1.88280	0.00000	-2.51040

atomic values (ε_a, ε_b) and (σ_a, σ_b) using the geometric combining rule

$$\varepsilon_{ab} = \sqrt{(\varepsilon_a \varepsilon_b)} \quad ; \quad \sigma_{ab} = \sqrt{(\sigma_a \sigma_b)} \tag{6}$$

The OPLS-AA model parameters for the atoms of the alcohols of this work are given in Tables 1–4. Alcohol sites will be hereafter denoted by H_{OH} (hydrogen of the hydroxyl group), O_{OH} (oxygen of the hydroxyl group), C (carbon site), and H (hydrogen linked to a carbon site). Note that the partial charge assigned to each carbon site depends on its bonding environment, i.e., it will differ according the number of H, and O directly linked to it.

{*Water-Water*}.The TIP4P/2005f is the flexible version of the well-known TIP4P/2005 model of Abascal and Vega [70]. It is known to reproduce correctly the experimental temperature of maximum density of water, as well as many other structural and thermodynamic properties. Preliminary calculations carried by us have shown that it is more suitable than its rigid counterpart to reproduce the pressure dependence of the TMD. Like the TIP4P model, it consists of four interactions sites, three representing the atoms of the water molecule (O_W for the oxygen and H_W for the hydrogen), and an auxiliary fourth site (M-site) along the bisector of the bond angle, $\theta = H_w - \widehat{O_w} - H_w$. The O_W site consists of a Lennard-Jones center with $\varepsilon_{O_W}/\kappa_B$ = 93.2 K and σ_{O_W} = 0.31644 nm, the H_W is a bare point charge with $q_{H_{W_i}} = 0.5564\,e$, and finally, the auxiliary M-site is also a bare point charge, $q_M = -1.1128\,e$ with a variable separation from the O_W site, given by $r_{O_W-M} = 0.13194(z_{O_W-H_{W_1}} + z_{O_W-H_{W_2}})$ with $z_{O_W-H_{W_i}} = r_{O_W-H_{W_i}}\cos(\theta/2)$, where $r_{O_W-H_{W_i}}$ is the bond distance between the O_W and H_W sites. The bonded contribution to the potential energy U^W_{bonded}consists of two terms

$$U^W_{bonded} = U^W_{bond} + U^W_{angle} \tag{7}$$

$$U^W_{bond} = \sum_{i=1}^{2} D_r\left[1 - \exp\left(-\beta\left(r_{O_W-H_{W_i}} - r^0_{O_W-H_{W_i}}\right)^2\right)\right] \tag{8}$$

$$U^W_{angle} = \frac{1}{2}k_\theta\left(\theta - \theta^0\right)^2 \tag{9}$$

where D_r= 432.581 kJ·mol^{-1}, $r^0_{O_W-H_{W_i}} = 0.9419$ nm, k_θ = 367.810 kJ·mol^{-1}·rad^{-1}, and θ^0 = 107.4°. The non-bonded interaction between water molecules $U^W_{nonbonded}$ is given by eq. (5) with the corresponding Lennard-Jones and partial charges of the TIP4P/2005f model.

{*Alcohol-Water*}. The non-bonded interaction between alcohol and water molecules, $U^{AW}_{nonbonded}$,follows also Eq. (5) with the Lennard-Jones cross parameters between O_W and the corresponding LJ centers of the alkyl group atoms of alcohols calculated using the geometric combining rule – Eq. (6)–. As mentioned, the cross terms between the O_W sites and O_{OH} site of alcohols are fitted to reproduce the experimental excess properties, following the procedure described below.

2.2. Fitting procedure

Both $\varepsilon_{O_W-O_{OH}}$ and $\sigma_{O_W-O_{OH}}$, were optimized to obtain the best fit of the experimental excess enthalpy, h^E, and the excess volume, v^E, at 298.15 K and 1 bar over the whole composition range following the scheme:

i) Initial guesses for $\varepsilon_{O_W-O_{OH}}$ and $\sigma_{O_W-O_{OH}}$ are set using the geometric combining rule – Eq. (6)–, denoted as $\varepsilon^{GM}_{O_W-O_{OH}}$ and $\sigma^{GM}_{O_W-O_{OH}}$. A series of molecular simulations from low to high alcohol concentrations were run and both the excess enthalpy and excess volume are evaluated at specific alcohol mole fraction, *x*, denoted as $h^E(x; \varepsilon^{GM}_{O_W-O_{OH}}, \sigma^{GM}_{O_W-O_{OH}})$ and $v^E(x; \varepsilon^{GM}_{O_W-O_{OH}}, \sigma^{GM}_{O_W-O_{OH}})$.

ii) The same type of molecular simulations were also run changing the parameter values by finite differences as $\varepsilon^{GM}_{O_W-O_{OH}} \pm \Delta\varepsilon$ and $\sigma^{GM}_{O_W-O_{OH}} \pm \Delta\sigma$ in order to evaluate the series of excess properties at each alcohol mole fraction, *x*, $h^E(x; \varepsilon^{GM}_{O_W-O_{OH}} \pm \Delta\varepsilon, \sigma^{GM}_{O_W-O_{OH}})$, $v^E(x; \varepsilon^{GM}_{O_W-O_{OH}} \pm \Delta\varepsilon, \sigma^{GM}_{O_W-O_{OH}})$, $h^E(x; \varepsilon^{GM}_{O_W-O_{OH}}, \sigma^{GM}_{O_W-O_{OH}} \pm \Delta\sigma)$, and$v^E(x; \varepsilon^{GM}_{O_W-O_{OH}}, \sigma^{GM}_{O_W-O_{OH}} \pm \Delta\sigma)$.

iii) These quantities are used to evaluate the derivatives of the h^E and v^E with respect to $\varepsilon_{O_W-O_{OH}}$ and $\sigma_{O_W-O_{OH}}$ at mole fraction *x* by using centered differences, *e.g.*

$$\left(\frac{\partial h^E(x)}{\partial \varepsilon_{O_W-O_{OH}}}\right) = \frac{h^E\left(x; \varepsilon^{GM}_{O_W-O_{OH}} + \Delta\varepsilon, \sigma^{GM}_{O_W-O_{OH}}\right) - h^E\left(x; \varepsilon^{GM}_{O_W-O_{OH}} - \Delta\varepsilon, \sigma^{GM}_{O_W-O_{OH}}\right)}{2\Delta\varepsilon} \tag{10}$$

iv) Using a first order Taylor expansion around $\varepsilon^{GM}_{O_W-O_{OH}}$ and $\sigma^{GM}_{O_W-O_{OH}}$ one obtains a first approximation to the functional dependency of the h^E and v^E on $\varepsilon_{O_W-O_{OH}}$ and $\sigma_{O_W-O_{OH}}$ as

$$h^{E}\left(x;\varepsilon_{O_W-O_{OH}},\sigma_{O_W-O_{OH}}\right) = h^{E}\left(x;\varepsilon^{GM}_{O_W-O_{OH}},\sigma^{GM}_{O_W-O_{OH}}\right) + \left(\frac{\partial h^{E}(x)}{\partial\varepsilon_{O_W-O_{OH}}}\right)\left(\varepsilon_{O_W-O_{OH}}-\varepsilon^{GM}_{O_W-O_{OH}}\right) + \left(\frac{\partial h^{E}(x)}{\partial\sigma_{O_W-O_{OH}}}\right)\left(\sigma_{O_W-O_{OH}}-\sigma^{GM}_{O_W-O_{OH}}\right) \quad (11)$$

$$v^{E}\left(x;\varepsilon_{O_W-O_{OH}},\sigma_{O_W-O_{OH}}\right) = v^{E}\left(x;\varepsilon^{GM}_{O_W-O_{OH}},\sigma^{GM}_{O_W-O_{OH}}\right) + \left(\frac{\partial v^{E}(x)}{\partial\varepsilon_{O_W-O_{OH}}}\right)\left(\varepsilon_{O_W-O_{OH}}-\varepsilon^{GM}_{O_W-O_{OH}}\right) + \left(\frac{\partial v^{E}(x)}{\partial\sigma_{O_W-O_{OH}}}\right)\left(\sigma_{O_W-O_{OH}}-\sigma^{GM}_{O_W-O_{OH}}\right) \quad (12)$$

v) A least squares residue is constructed using the expressions above and the experimental values for the set of mole fractions under consideration. Then a Levenberg-Marquardt algorithm is used to determine the optimum values of $\varepsilon_{O_W-O_{OH}}$ and $\sigma_{O_W-O_{OH}}$ that minimize the objective residue function

$$\Phi = \sum_{x=0}^{1}\left[h^{E}\left(x;\varepsilon_{O_W-O_{OH}},\sigma_{O_W-O_{OH}}\right)-h^{E}_{exp}(x)\right]^2 + \sum_{x=0}^{1}\left[v^{E}\left(x;\varepsilon_{O_W-O_{OH}},\sigma_{O_W-O_{OH}}\right)-v^{E}_{exp}(x)\right]^2 \quad (13)$$

where subindex exp refers to experimental values.

vi) Molecular simulations are performed with the values resulting from the fit in step *v*), $\varepsilon_{O_W-O_{OH}}$ and $\sigma_{O_W-O_{OH}}$. If the new simulated excess properties are not satisfactory when compared to the experimental values the procedure returns to step *ii*) using now the results from the fit as initial estimates, and the scheme is repeated until the desired convergence is attained.

2.3. Simulation details

NpT molecular dynamics simulations in a cubic box under periodic boundary conditions were performed with a time step of 1 fs using GROMACS/2018.3 software package [71]. Temperature and pressure were fixed using the Nose-Hoover thermostat [72,73] and the isotropic Parrinello-Rahman barostat [74,75], with relaxation times of 2 ps. Coulombic interaction contributions were evaluated using the particle mesh Ewald (PME) method [76] using a 0.1 nm mesh and a fourth-order interpolation for the Fourier component of Ewald summations. The real part of the Ewald sums and Lennard-Jones interactions were truncated at 1.0 nm; standard LJ long-range corrections were included. The initial configuration was built using the insert-molecules module of GROMACS/2018.3 with the initial molecular structure of alcohols and water generated with the MOLDEN package [77]. Three series of simulations were performed in order to obtain an equilibrated configuration at each thermodynamic state (T, 1 bar, x): an initial NVT run using as starting point the initial configuration, a second NpT run at 100 bar, and finally an expansion NpT run at 1 bar. The initial configurations in the last two steps were the final configurations of the previous steps. Each of these simulations were 1 ns long. At each thermodynamic state (T, 1 bar, x) one production run 10 ns long was carried out using the equilibrated configuration as starting point. The averaged enthalpy and the volume were computed for subsequent calculations. Statistical uncertainties were estimated using the block average method obtaining averaged values of 0.02 kJ·mol^{-1} and 0.02 cm^3·mol^{-1}.

Excess enthalpy h^E and volume v^E (section 3.1) were computed from the simulated enthalpy h and volume v through the following relations

$$h^{E} = h - xh^{A} - (1-x)h^{W} \quad (14)$$

Table 5
Lennard-Jones cross parameters between oxygen of the OPLS-AA alcohols O_{OH} and oxygen O_W of TIP4P/2005f water.

Alcohol	$\varepsilon_{O_W-O_{OH}}$ (kJ·mol^{-1})	$\sigma_{O_W-O_{OH}}$ (nm)
methanol	0.96970	0.31118
ethanol	0.78375	0.31487
1-propanol	0.72268	0.31633
2-propanol	0.77944	0.31455
tert-butanol	0.71554	0.31602

$$v^{E} = v - xv^{A} - (1-x)v^{W} \quad (15)$$

where *A* and *W* denote pure alcohol and water respectively. Excess properties were computed from runs of 500 molecule samples at alcohol mole fractions x= 0.05, 0.1, 0.2, 0.3, 0.4, 0.5, 0.6, 0.7, 0.8, and 0.9, in addition to runs for the pure substances, all at 298.15 K and 1 bar. For the calculation of the TMD (section 3.2) we have used 2000 molecule samples at alcohol mole fractions x= 0.005, 0.015, 0.025, and at temperatures 250, 260, 270, 280, 290, 300, 310, 320, and 330 K, and with the pressure set to 1 bar.

3. Results and discussion

3.1. Excess properties: Lenard-Jones cross parameters determination

3.1.1. A worked example: {methanol + water}

Excess molar enthalpies $h^{E,}$ and excess molar volumes $v^{E,}$ for the {methanol+water} binary system at atmospheric pressure and 298.15 K were experimentally determined by Lama and Lu [78] and by Benson and Kiyohara [79], respectively. These data are plotted in Figure 1 as full lines. Both excess properties take negative values over the whole composition range; the h^E – x curve displays a minimum at low mole fractions, whereas in the v^E – x curve the minimum appears close to the equimolar composition. Experimental data are compared in Figure 1 with simulation results obtained using the geometric combining rule for all the LJ cross parameters (results of step *i* of the fitting procedure). The standard uncertainties in simulated h^E and v^E were estimated around 0.03 kJ·mol^{-1} and 0.03 cm^3·mol^{-1}, respectively. As it can be seen, v^E is well described by simulations, but the simulated h^E deviates considerably from the experimental data, with the minimum shifted towards a much higher mole fraction. Clearly, there is room for improvement, so then we move to the fitting procedure.

Starting from the geometric mean estimates, the different stages of the first iteration of the optimization procedure are illustrated in Figure 2. After a couple of iterations the optimal values obtained were $\varepsilon_{O_W-O_{OH}}$= 0.96970 kJ·mol^{-1} $\sigma_{O_W-O_{OH}}$= 0.31118 nm, which now lead to accurate h^E and v^E values, as illustrated in Figure 3.

3.1.2. Other {alcohol+water} systems

The same procedure described above for methanol aqueous solutions was used to obtain the fitted LJ cross parameters between water's oxygen O_W and that of the hydroxyl group O_{OH} for {ethanol, 1-propanol, 2-propanol, and tert-butanol + water} binary systems. Experimental excess enthalpies h^E were reported by Lama and Lu [78] (ethanol, 2-propanol solutions), by Davis and Ham. [80] (1-propanol), and by Koga [81–83] (tert-butanol). Experimental excess molar volumes v^E were measured by Benson and Kiyohara [79] (ethanol and 1-propanol), Davis and Ham [80] (2-propanol), and Kipkemboi and Easteal [84] (tert-butanol). The final values of $\varepsilon_{O_W-O_{OH}}$ and $\sigma_{O_W-O_{OH}}$ are reported in Table 5.

Figure 4 shows the h^E values obtained by simulation using parameters of Table 5 plotted as a function of alcohol mole frac-

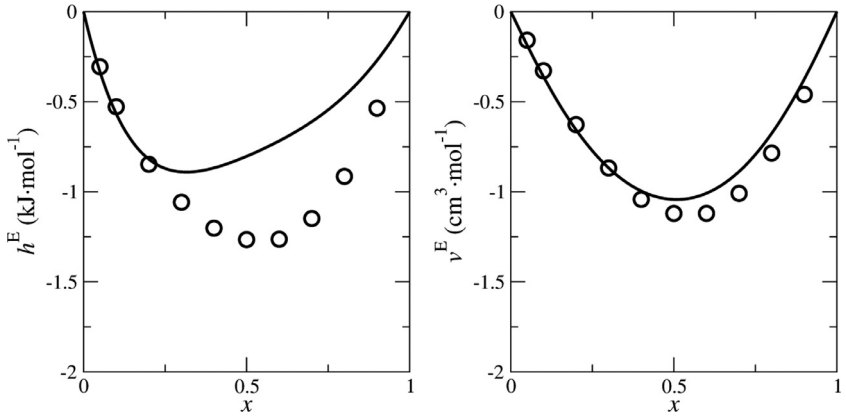

Figure 1. Excess molar enthalpy h^E (left) and excess molar volume v^E (right) for the {methanol + water} binary system plotted as a function of methanol mole fraction x. Full line are experimental data and points are simulation data obtained using $\varepsilon_{O_W-O_{OH}} = 0.742409$ kJ·mol^{-1} and $\sigma_{O_W-O_{OH}} = 0.314212$ nm.

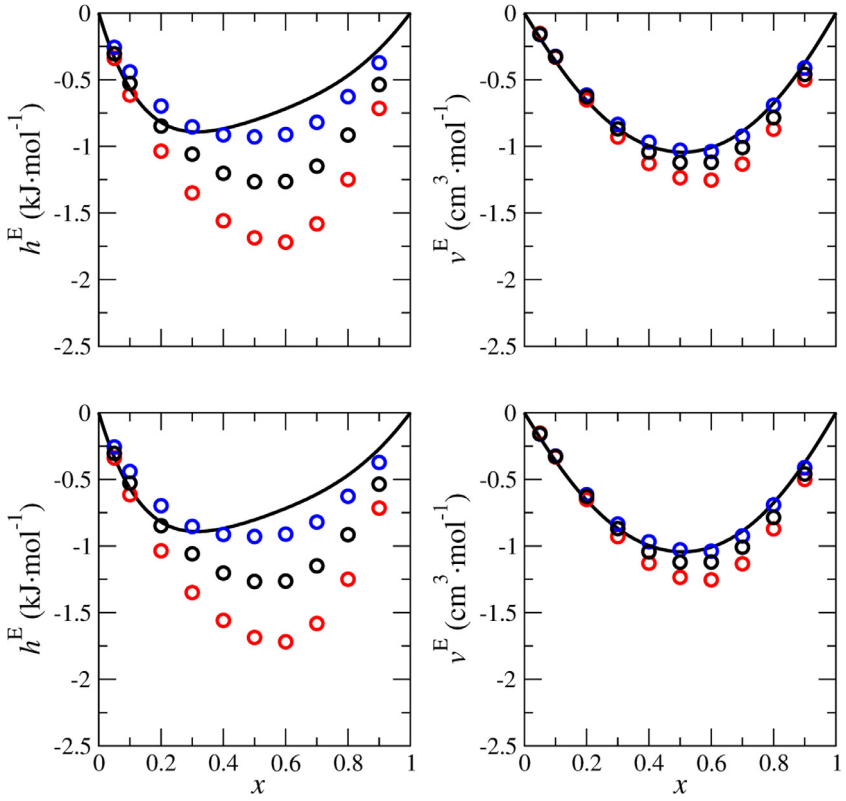

Figure 2. Excess molar enthalpy h^E (left) and excess molar volume v^E (right) for the {methanol + water} binary system plotted as a function of methanol mole fraction x. Full line are experimental data and points are simulation data. Upper graphics: $\sigma_{O_W-O_{OH}} = 0.314212$ nm and (red) $\varepsilon_{O_W-O_{OH}}$ =0.702409 kJ·mol^{-1}, (black) $\varepsilon_{O_W-O_{OH}}$ =0.742409 kJ·mol^{-1}, and (blue) $\varepsilon_{O_W-O_{OH}}$ =0.782409 kJ·mol^{-1}. Lower graphics: $\varepsilon_{O_W-O_{OH}} = 0.742409$ kJ·mol^{-1}, and (red) $\sigma_{O_W-O_{OH}}$ =0.312212 nm, (black) $\sigma_{O_W-O_{OH}}$ =0.314212 nm, and (blue) $\sigma_{O_W-O_{OH}}$ =0.316212 nm.

tion x for all binary mixtures under consideration, and compared with experimental data. As it can be seen, the shape of the experimental h^E-x curves is well described by these simulations, exhibiting a proper location of the minima and maxima at low and high alcohol concentrations, respectively. A good quantitative agreement is found in all cases. Figure 5 collects all the simulated v^E data compared with experimental results. In this case, a very good description is also attained for systems containing ethanol, 1-propanol and 2-propanol. In contrast, simulation v^E results for aqueous solutions of tert-butanol are consistently above the experimental values for x>0.2 . Further iterations of the fitting procedure did not improve the results, which seems to suggest that other cross LJ interactions (*e.g.* O_W-C) might have to be included in the optimization procedure in order to fix this shortcoming.

Exploring the possibility of defining a common set of LJ parameters for short-chain alcohols,we found $\varepsilon_{O_W-O_{OH}} = 0.7$ kJ·mol^{-1}; $\sigma_{O_W-O_{OH}} = 0.317$ *nm*. These values were determined after observing that similar simulation results are found if the fully optimized LJ parameters are slightly modified by decreasing $\varepsilon_{O_W-O_{OH}}$ and increasing $\sigma_{O_W-O_{OH}}$, simultaneously. Simulation results using these LJ parameters were found to lie very close to those obtained from the optimized parameters for all alcohols mixtures with the sole exception of the excess enthalpy of methanol/water (with slightly higher values), as can be seen in the Supplementary Material. For the sake of simplicity and without a great loss of pre-

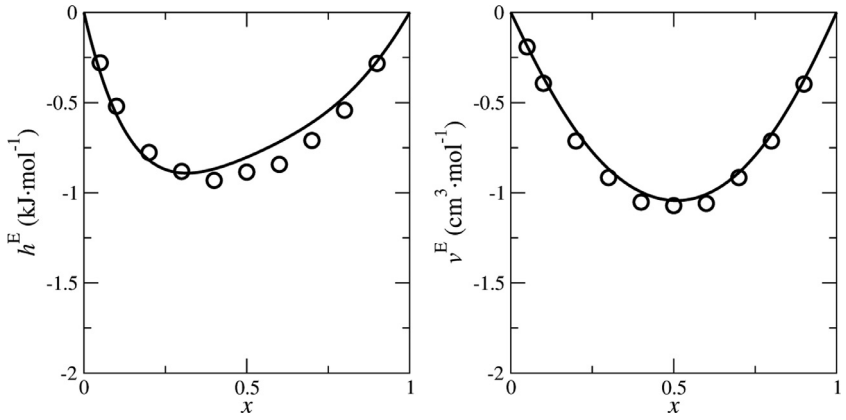

Figure 3. Excess molar enthalpy h^E (left) and excess molar volume v^E (right) for the {methanol + water} binary system plotted as a function of methanol mole fraction x. Full line are experimental data and points are simulation data obtained using $\varepsilon_{O_W-O_{OH}}$ =0.96970 kJ·mol^{-1} and $\sigma_{O_W-O_{OH}}$ =0.31118 nm.

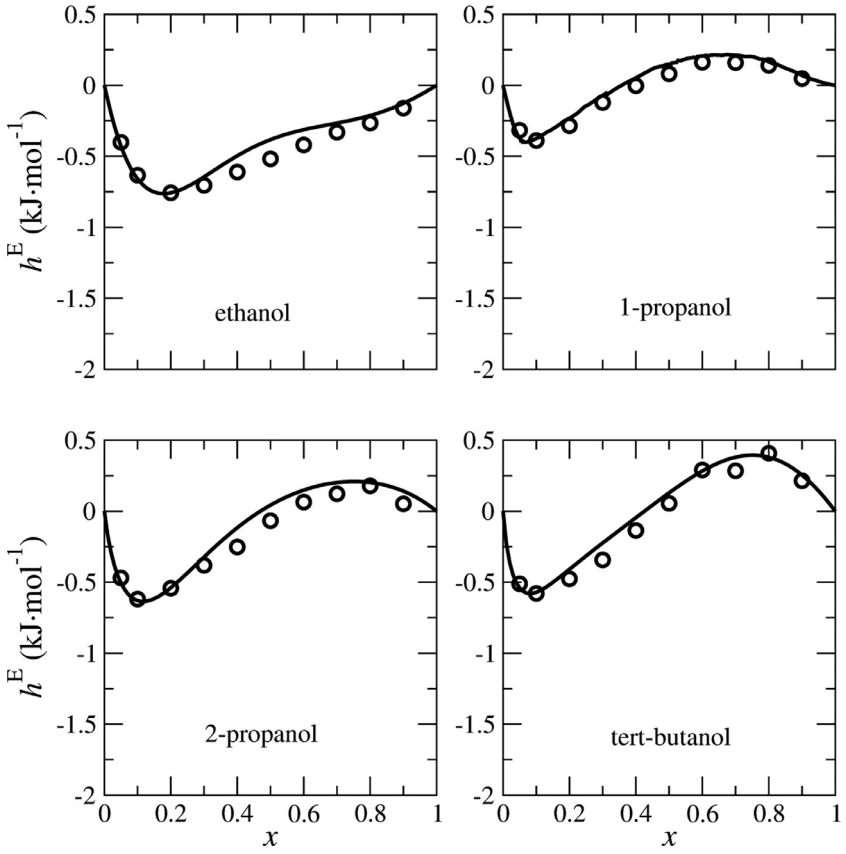

Figure 4. Excess molar enthalpy h^E for several {alcohol+ water} binary systems plotted as a function of alcohol mole fraction x. Full line are experimental data and points are simulation data obtained using $\varepsilon_{O_W-O_{OH}}$ = 0.78375 kJ·mol^{-1} and $\sigma_{O_W-O_{OH}}$ = 0.31487 nm (ethanol), $\varepsilon_{O_W-O_{OH}}$ = 0.72268 kJ·mol^{-1} and $\sigma_{O_W-O_{OH}}$ = 0.31633 nm (1-propanol), $\varepsilon_{O_W-O_{OH}}$ = 0.77944 kJ·mol^{-1} and $\sigma_{O_W-O_{OH}}$ =0.31455 nm (2-propanol), and $\varepsilon_{O_W-O_{OH}}$ = 0.71554 kJ·mol^{-1} and $\sigma_{O_W-O_{OH}}$ = 0.31602 nm (tert-butanol).

cision, these values can be alternatively used instead of those given in Table 5 for aqueous mixtures of ethanol, 1-propanol, 2-propanol and tertbutanol.

3.2. Temperature of maximum density

Densities ρ obtained by isothermal-isobaric simulations using the model parameters of Table 5 at atmospheric pressure for our binary systems at alcohol mole fractions x= 0.005, 0.015, and 0.025 and for pure water are plotted in Figure 6 as a function of temperature T. Black circles in the upper part of each graph correspond to pure water results (TIP4P/2005f model) which follow very accurately the experimental ρ -T curve (also shown as a black line [85]), as was previously found by González *et al.* [69]. Addition of small amounts of alcohol reduces the sample density to different degree depending on the type of alcohol, shifting the TMD to values lower than that of pure water. A quantitative estimation of TMD was performed by fitting the ρ -T data to a third degree polynomial ($\rho = A + B \cdot T + C \cdot T^2 + D \cdot T^3$) and solving $d\rho/dT = B + 2C \cdot T + 3D \cdot T^2 = 0$. The resulting TMDs are presented in Table 6. The standard uncertainty of the TMD evaluation was estimated in 1 K. Figure 6 also shows experimental density values [79,80,84] at x = 0.025 and 298.15 K for all the systems. As can be seen, a good agreement was found com-

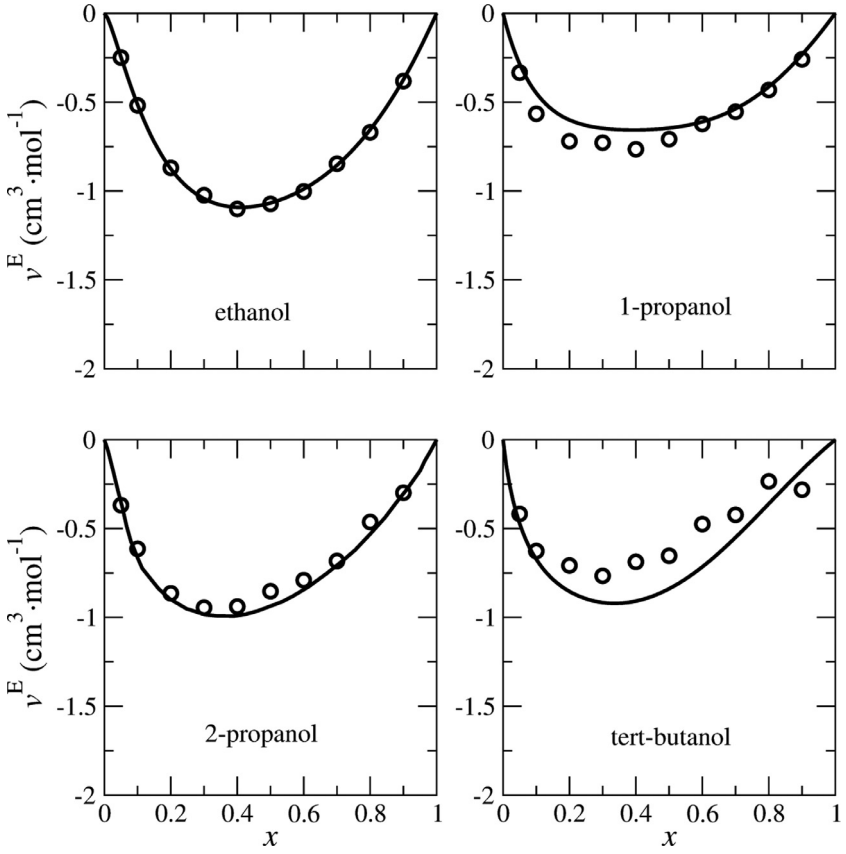

Figure 5. Excess molar volume v^E for several {alcohol+ water} binary systems plotted as a function of alcohol mole fraction x. Full line are experimental data and points are simulation data obtained using $\varepsilon_{O_W-O_{OH}}$ = 0.78375 kJ·mol^{-1} and $\sigma_{O_W-O_{OH}}$= 0.31487 nm (ethanol), $\varepsilon_{O_W-O_{OH}}$ = 0.72268 kJ·mol^{-1} and $\sigma_{O_W-O_{OH}}$ = 0.31633 nm (1-propanol), $\varepsilon_{O_W-O_{OH}}$ = 0.77944 kJ·mol^{-1} and $\sigma_{O_W-O_{OH}}$ =0.31455 nm (2-propanol), and $\varepsilon_{O_W-O_{OH}}$ = 0.71554 kJ·mol^{-1} and $\sigma_{O_W-O_{OH}}$ = 0.31602 nm (tert-butanol).

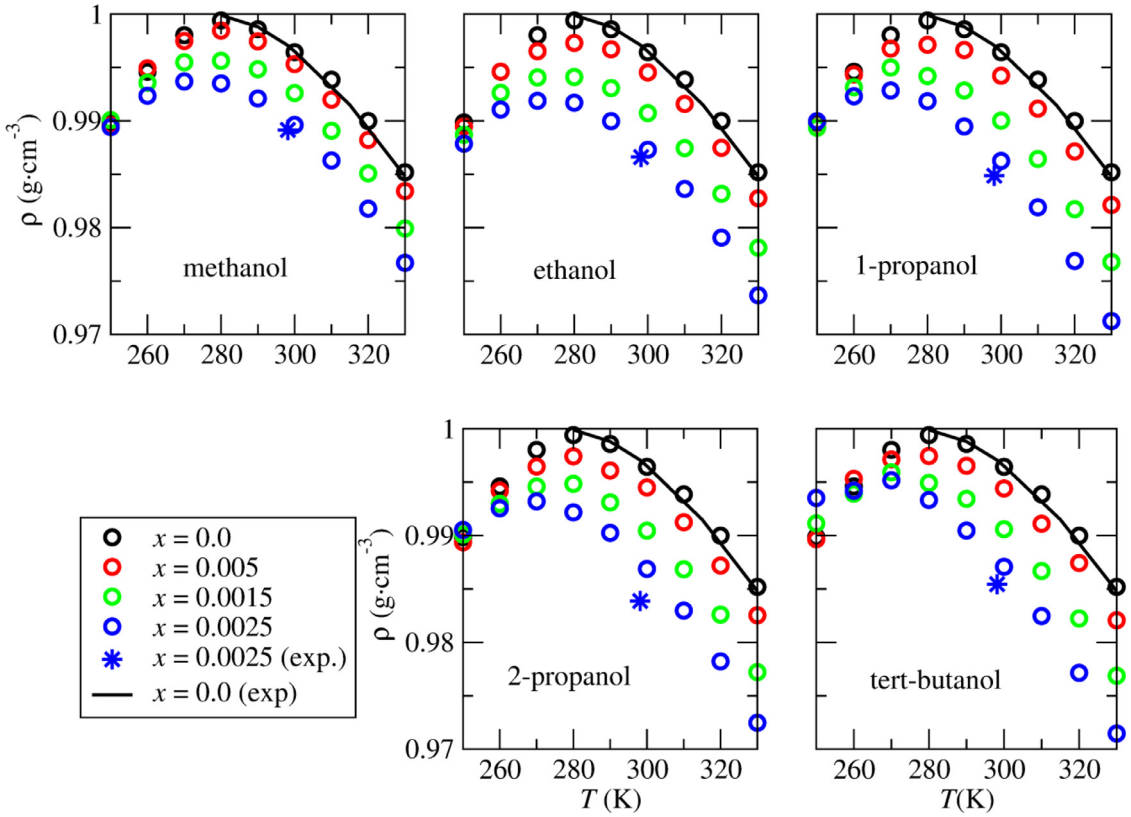

Figure 6. Densities ρ plotted as a function of temperature T for pure water and diluted aqueous solutions of alcohols of mole fraction x obtained by simulation using parameters of Table 5 and from experiments [79,80,84,85].

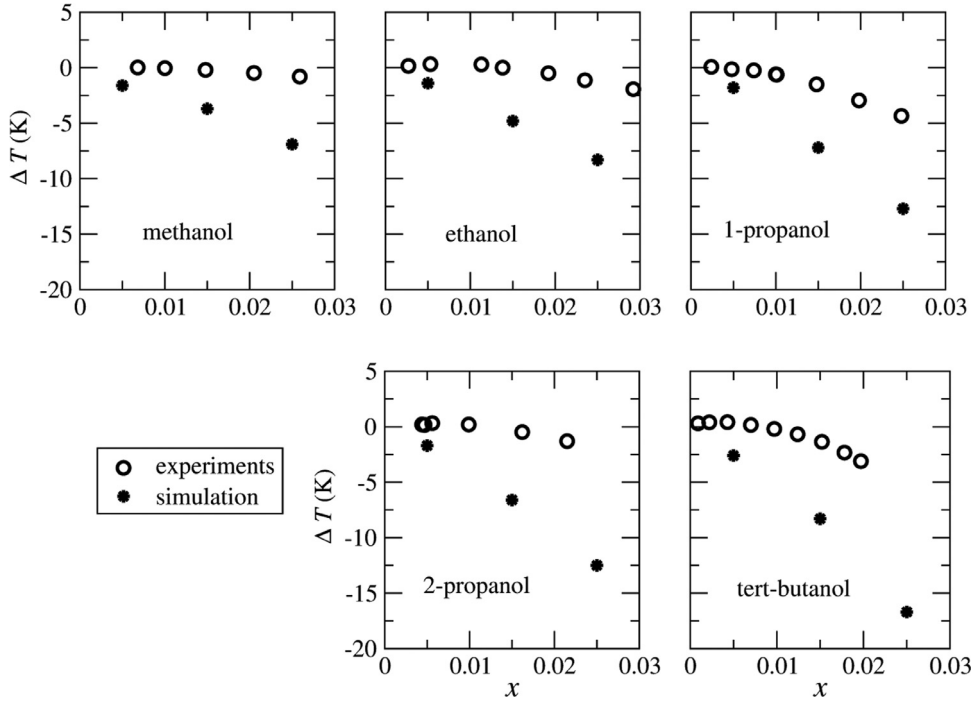

Figure 7. Difference between the temperature of maximum density of diluted aqueous solutions of alcohols and that of pure water ΔT plotted as a function of alcohol mole fraction x. Simulation data were obtained using parameters of Table 5. Experimental data were taken from reference [12].

Table 6
Temperature of maximum density TMD for several aqueous solutions of alcohols of mole fraction x at atmospheric pressure obtained by simulation. TMD for pure water (TIP4P/2005f) is 281.5 K.

	TMD (K)				
	methanol	ethanol	1-propanol	2-propanol	tertbutanol
$x = 0.005$	279.9	280.1	279.7	279.8	278.9
$x = 0.015$	277.8	276.7	274.3	274.9	273.2
$x = 0.025$	274.6	273.2	268.8	269	264.8

Table 7
Despretz constant, K_x and K_c, of the aqueous solutions of alcohols obtained from simulations.

Solute	$K_x \pm \sigma\_K_x$ (K)	$K_c \pm \sigma\_K_c$ (K·mg^{-1}·g)
methanol	-269 ± 9	-0.1484 ± 0.0048
ethanol	-327 ± 6	-0.1253 ± 0.0018
1-propanol	-497 ± 16	-0.1456 ± 0.0041
2-propanol	-480 ± 21	-0.1408 ± 0.0056
tert-butanol	-634 ± 31	-0.1509 ± 0.0070

pared to the simulation results except maybe for the 2-propanol mixture.

The change in the TMD of water due to the addition of alcohol, ΔT = TMD (mixture) -TMD (pure water), is plotted in Figure 7 as a function of alcohol mole fraction, x, for all the systems under study. Experimental data from Wada and Umeda [12] are included in the figure for comparison. One immediately appreciates that the simulated ΔT exhibits a monotonic decrease considerably more pronounced than that of the final section of the experimental curves. In all instances, the maxima in ΔT *vs* x for very dilute solutions present in the experimental results, is missing in our simulations. This is in agreement with the findings of previous works [67,86] where we observed the same behavior for diluted aqueous solutions of methanol [67] and amino acids [86]. Thus, the "structure maker" character experimentally found for these short-chain alcohols is not captured by our models. This means that even potential models able to capture the experimental behavior of molar excess properties over the whole concentration range, fail to account for the subtle effect that these short chain alcohols have on the structure of water. One must however stress, that, despite being subtle, this effect leads to a qualitatively different behavior of the TMD curves.

All simulated ΔT data are plotted together in Figure 8 as a function of alcohol mole fraction, x,(left) and mass concentration, c, –mg alcohol/gram of water– (right). The variation of ΔT *vs* x presents a strong correlation with the alcohol molar mass (methanol, 32.04 g, ethanol, 46.07 g, propanol, 60.09 g, and tert-butanol, 74.12 g); in other words, the higher the molar mass the stronger the change in ΔT with x. This molar mass effect is no longer visible if ΔT is plotted against mass concentration, c (left graph of Fig. 8). As can be seen, all data approximately collapse into the same curve. This actually means that, in the simulated results, the only factor that determines differences in the behavior of different alcohols is the size of the alkyl chain, and actually, the dependence of ΔT on its molar mass is linear.

A quantitative assessment of this effect can be attained by fitting the ΔT data to the Despretz equation [87], $\Delta T = K_y \cdot y$, where K_y is the Despretz constant, and y can be either the alcohol mole fraction, x, or its mass concentration, c. Results are collected in Table 7. The K_c values are lying in the interval (-0.015, -0.013) K·mg^{-1}·g, and are rather similar to those previously obtained for aminoacids in water [86] (-0.012, -0.010) K·mg^{-1}·g, which were also determined using the OPLS-AA force field. These results suggest a slightly stronger change of ΔT with concentration for short chain alcohols as compared to aminoacids solutions, which contradicts the experimental results [12,86]. Somehow, in contrast with the experimental behavior, our OPLS-AA models overestimate the "structure breaker" character of short-chain alcohol, and miss completely the "structure maker" effect experimentally found at very high dilutions.

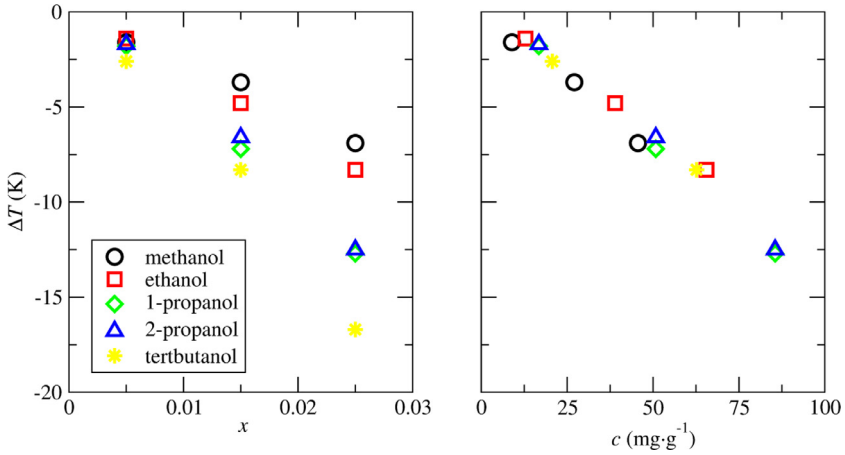

Figure 8. Difference between the temperature of maximum density of diluted aqueous solutions of alcohols and that of pure water ΔT plotted as a function of alcohol mole fraction x (left) and mass concentration c (right). All results are simulation data obtained using parameters of Table 5.

4. Conclusions

Extensive NpT MD simulations of aqueous solutions of methanol, ethanol, 1-propanol, 2-propanol, and tert-butanol at atmospheric pressure and at 298.15 K were performed. Alcohols were modeled using the OPLS-AA force field and water was described by using the flexible version of the TIP4P/2005 model. The Lennard-Jones cross interactions between alcohol and water sites were defined using the geometric combining rule except those between the oxygen sites of water and alcohols which were fitted to reproduce the experimental excess enthalpy, h^E, and excess molar volume, v^E. Simulation results with the proposed parametrization yield an accurate description of h^E and v^E for all systems, with only some discrepancies for the v^E of aqueous solutions of tert-butanol. Interestingly, for alcohols with alkyl chains longer than that of methanol, $\varepsilon_{O_W-O_{OH}} = 0.7\,\mathrm{kJ\cdot mol^{-1}}$; $\sigma_{O_W-O_{OH}} = 0.317\,\mathrm{nm}$ lead to very similar simulation results compared to those obtained with the fully optimized parameters. These values should be a better choice than the use of plain mixing rules. The effect of the addition of small amounts of these alcohols on the temperature of maximum density of water was studied using this parametrization and compared with experimental data. Simulations were performed at atmospheric pressure and in the temperature interval (250-330) K. The experimental increase of the TMD at very low alcohol concentrations was not reproduced by the simulation results. Consequently, our model fails to properly capture the experimental "structure maker" character of short-chain alcohols. In all the cases, simulated TMDs decreases strongly with concentration, overestimating the experimental Despretz constants, K_c. These are very similar with values lying in the interval (-0.015, -0.013) $K\cdot mg^{-1}\cdot g$.

Despite the good quality of our models for the excess thermodynamics of mixtures over the whole composition range, they cannot account for the subtle influence of the presence of small amounts of these alcohols solutes on the TMD of water. The inclusion of flexibility in our models does not improve the results when compared with those previously obtained for rigid models [64]. Clearly, one needs to consider most likely non-additive effects such as those of polarizability and/or charge transfer, and produce a more accurate representation of the peculiar nature of hydrogen bonding in order to overcome the shortcomings of the present models.

Declaration of Competing Interest

None.

CRediT authorship contribution statement

Encarnación García Pérez: Methodology, Software, Formal analysis, Investigation. **Diego González-Salgado:** Conceptualization, Methodology, Software, Validation, Formal analysis, Writing - original draft. **Enrique Lomba:** Conceptualization, Supervision, Writing - review & editing.

Acknowledgments

Authors acknowledge funding from the Fondo Europeo de Desarrollo Regional (FEDER) and the Agencia Estatal de Investigación (AEI) under grant no. FIS2017-89361-C3-3-P.

Supplementary materials

Supplementary material associated with this article can be found, in the online version, at doi:10.1016/j.fluid.2020.112840.

References

[1] K.G. Zhou, N.-N. Mao, H.-X. Wang, Y. Peng, H.-L. Zhang, A mixed-solvent strategy for efficient exfoliation of inorganic graphene analogues, Angew. Chem. Int. Ed. 50 (2011) 10839–10842.
[2] X. Jiang, Y. Wang, M. Li, Selecting water-alcohol mixed solvent for synthesis of polydopamine nano-spheres using solubility parameter, Scientific Reports 4 (2015) No. 6070.
[3] C.R. Smith, Alcohol as a disinfectant against the tubercle bacillus, Public Health Rep 62 (1947) 1285–1295.
[4] J.A. Duffie, W.A. Beckman, Solar Engineering of Thermal Processes, Wiley, New York, 1992.
[5] J.B. Jaimes, M. Alvarez, J.V. Rojas, R.M. Filho, Pervaporation: Promissory Method for the Bioethanol Separation of Fermentation, Chem. Eng. Trans. 38 (2014) 139–144.
[6] M.O. Dias, T.L. Junqueira, C.E.V. Rossell, R.M. Filho, A. Bonomi, Evaluation of process configurations for second generation integrated with first generation bioethanol production from sugarcane, Fuel Process. Technol. 109 (2013) 84–89.
[7] F. Franks, D.J.G. Ives, The structural properties of alcohol-water mixtures, Quat. Rev. Chem. Soc. 20 (1966) 1–44.
[8] F. Franks, J.E. Desnoyers, in: F. Franks (Ed.), Water Science Reviews, 1, Cambridge University Press, Cambridge, 1985, pp. 171–232.

[9] H.S. Frank, M.W. Evans, Free volume and entropy in condensed systems. III.Entropy in binary liquid mixtures; partial molal entropy in dilute solutions;structure and thermodynamics in aqueous electrolytes, J. Chem. Phys. 13 (1945) 507–532.
[10] N. Galamba, Water's Structure around Hydrophobic Solutes and the Iceberg Model, J. Phys. Chem. B 117 (2013) 2153–2159.
[11] S. Dixit, J. Crain, W.C.K. Poon, J.L. Finney, A.K. Soper, Molecular segregation observed in a concentrated alcohol-water solution, Nature 416 (2002) 829–832; L. Dougan, S.P. Bates, R. Hargreaves, J.P. Fox, J. Crain, J.L. Finney, V. Reat, A.K. Soper, Methanol-water solutions: a bi-percolating liquid mixture, J. Chem. Phys. 121 (2004) 6456–6462; I. Bakó, L. Pusztai, L. Temleitner, Decreasing temperature enhances the formation of sixfold hydrogen bonded rings in water-rich water-methanol mixtures, Sci. Rep. 7 (2017) No. 1073; A. Perera, Molecular emulsions: from charge order to domain order, Phys. Chem. Chem. Phys. 19 (2017) 28275–28285.
[12] G. Wada, S. Umeda, Effects of nonelectrolytes on the temperature of the maximum density of water. I. Alcohols, Bull. Chem. Soc. Jpn. 35 (1962) 646–652.
[13] G. Wada, S. Umeda, Effects of nonelectrolytes on the temperature of the maximum density of water. II. Organic compounds with polar groups, Bull. Chem. Soc. Jpn. 35 (1962) 1797–1801.
[14] E.W. Washburn, International Critical Tables, McGraw-HillBook Co. Inc, New York, 1933.
[15] A.P. Furlan, E. Lomba, M.C. Barbosa, Temperature of maximum density and excess properties of short-chain alcohol aqueous solutions: A simplified model simulation study, J. Chem. Phys. 146 (2017) No. 144503.
[16] M.P. Allen, D.J. Tildesley, Computer Simulation of Liquids, Oxford University Press, 1987.
[17] D. Frenkel, B. Smit, Understanding Molecular Simulation, Academic Press, London, 2002.
[18] V.M. Anisimov, I.V. Vorobyov, B. Roux, A.D. MacKerell, Polarizable Empirical Force Field for the Primary and Secondary Alcohol Series Based on the Classical Drude Model, J. Chem. Theory Comput. 3 (2007) 1927–1946.
[19] J. Dai, X. Li, L. Zhao, H. Sun, Enthalpies of mixing predicted using molecular dynamics simulations and OPLS force field, Fluid Phase Equilib 289 (2010) 156–165.
[20] D. Gonzalez-Salgado, I. Nezbeda, Excess properties of aqueous mixtures of methanol: simulation versus experiment, Fluid Phase Equilib 240 (2006) 161–166.
[21] J. Fidler, P.M. Rodger, Solvation Structure around Aqueous Alcohols, J. Phys. Chem. B 103 (1999) 7695–7703.
[22] J.L. Finney, D.T. Bowron, R.M. Daniel, P.A. Timmins, M.A. Roberts, Molecular and mesoscale structures in hydrophobically drivenaqueous solutions, Biophysical Chemistry 105 (2003) 391–409.
[23] M. Kiselev, D. Ivlev, The study of hydrophobicity in water–methanol and water–tert-butanol mixtures, J. Mol. Liq. 110 (2004) 193–199.
[24] A. Henao, A.J. Johnston, E. Guardia, S.E. McLain, L.C. Pardo, On the positional and orientational order of water and methanol around indole: a study on the microscopic origin of solubility Phys, Chem. Chem. Phys. 18 (2016) No. 23006.
[25] Z. Su, S.V. Buldyrev, P.G. Debenedetti, P.J. Rossky, H.E. Stanley, Modeling simple amphiphilic solutes in a Jagla solvent, J. Chem. Phys. 136 (2012) No. 044511.
[26] C. Nieto-Draghi, J. Bonet, B. Rousseau, Computing the Soret coefficient in aqueous mixtures using boundary driven nonequilibrium molecular dynamics, J. Chem. Phys. 122 (11) (2005) No. 114503.
[27] A. Perera, L. Zoranic, F. Sokolic, R. Mazighi, A comparative molecular dynamics study of water – methanol and acetone – methanol mixtures, J. Mol. Liq. 159 (2011) 52–59.
[28] I. Bakó, L. Pusztai, L. Temleitner, Decreasing temperature enhances the formation of sixfold hydrogen bonded rings in water-rich water-methanol mixtures, Sci. Rep. 7 (2017) No. 1073.
[29] J.T. Slusher, Infinite dilution activity coefficients in hydrogen-bonded mixtures via molecular dynamics: the water-methanol system, Fluid Phase Equilib 154 (1999) 181–192.
[30] G. Guevara-Carrion, J. Vrabec, H. Hasse, Prediction of self-diffusion coefficient and shear viscosity of water and its binary mixtures with methanol and ethanol by molecular simulation, J Chem Phys 134 (2011) No. 074508.
[31] E.J.W. Wensink, A.C. Hoffmann, P.J. van Maaren, D. van der Spoel, Dynamic properties of water-alcohol mixtures studied by computer simulation, J. Chem. Phys. 119 (2003) No. 7308.
[32] S. Pothoczki, L. Pusztai, I. Bakó, Temperature dependent dynamics in water-ethanol liquid mixtures, J. Mol. Liq. 271 (2018) 571–579.
[33] S. Pothoczki, L. Pusztai, I. Bakó, Variations of the Hydrogen Bonding and Hydrogen-Bonded Network in Ethanol–Water Mixtures on Cooling, J. Phys. Chem. B 122 (2018) 6790–6800.
[34] S. Banerjee, B. Bagchi, Stability of fluctuating and transient aggregates of amphiphilic solutes in aqueous binary mixtures: Studies of dimethylsulfoxide, ethanol, and tert-butyl alcohol, J. Chem. Phys. 139 (2013) No. 164301.
[35] S.Y. Noskov, G. Lamoureux, B. Roux, Molecular dynamics study of hydration in ethanol–water mixtures using a polarizable force field, J Phys Chem B 109 (2005) 6705–6713.
[36] K. Kholmurodov, E. Dushanov, K. Yasuoka, H. Khalil, A. Galal, S. Ahmed, N. Sweilam, H. Moharram, Molecular dynamics simulation of the interaction of ethanol-water mixture with a Pt surface, Natural Science 3 (2011) 1011–1021.
[37] S. Banerjee, R. Gosh, B. Bagchi, Structural Transformations, Composition Anomalies and a Dramatic Collapse of Linear Polymer Chains in Dilute Ethanol–Water Mixtures, J. Phys. Chem. B 116 (12) (2012) 3713–3722.
[38] M. Mijaković, B. Kežić, L. Zoranić, F. Sokolić, A. Asenbaum, C. Pruner, E. Wilhelm, A. Perera, Ethanol-water mixtures: ultrasonics, Brillouin scattering and molecular dynamics, J. Mol. Liq. 164 (2011) 66–73.
[39] M. Mijaković, K.D. Polok, B. Kežić, F. Sokolić, A. Perera, L. Zoranić, A comparison of force fields for ethanol – water mixtures, Molecular Simulation 41 (9) (2015) 699–712.
[40] A. Asenbaum, C. Pruner, E. Wilhelm, M. Mijakovic, L. Zoranic, F. Sokolic, B. Kezic, A. Perera, Structural changes in ethanol–water mixtures: Ultrasonics, Brillouin scattering and molecular dynamics studies, Vibrational Spectroscopy 60 (2012) 102–106.
[41] A. Klinov, I. Anashkin, Diffusion in Binary Aqueous Solutions of Alcohols by Molecular Simulation, Processes 7 (2019) No. 947.
[42] O. Gereben, L. Pusztai, Investigation of the Structure of Ethanol−Water Mixtures by Molecular Dynamics Simulation I: Analyses Concerning the Hydrogen-Bonded Pairs, J. Phys. Chem. B 119 (2015) 3070–3084.
[43] Y. Zhong, S. Patel, Electrostatic polarization effects and hydrophobic hydration in ethanol–water solutions from molecular dynamics simulations, J. Phys. Chem. 113 (2009) 767–778.
[44] C. Zhang, X. Yang, Molecular dynamics simulation of ethanol/water mixtures for structure and diffusion properties, Fluid Phase Equilib 231 (2005) 1–10.
[45] J.G. Méndez-Bermúdez, H. Dominguez, L. Pusztai, S. Guba, B. Horváth, I. Szalai, Composition and temperature dependence of the dielectric constant of 1-propanol/water mixtures: Experiment and molecular dynamics simulations, J. Mol. Liq. 219 (2016) 354–358.
[46] J.G. Méndez-Bermúdez, H. Dominguez, L. Temleitner, L. Pusztai, On the structure factors of aqueous mixtures of 1-propanol and 2-propanol: X-ray diffraction experiments and molecular dynamics simulations, Phys. Status Solidi B 255 (2018) No. 1800215.
[47] J.W. Bye, C.L. Freeman, J.D. Howard, G. Herz, J. McGregor, R.J. Falconer, Analysis of mesoscopic structured 2-propanol/water mixtures using pressure perturbation calorimetry and molecular dynamic simulation, J. Solution Chem. 46 (2017) 175–189.
[48] A. Idrissi, S. Longelin, The study of aqueous isopropanol solutions at various concentrations: low frequency Raman spectros- copy and molecular dynamics simulations, J. Mol. Struct. 651− 653 (2003) 271–275.
[49] S. Pothoczki, L. Pusztai, I. Bakó, Molecular Dynamics Simulation Studies of the Temperature- Dependent Structure and Dynamics of Isopropanol−Water Liquid Mixtures at Low Alcohol Content, J. Phys. Chem. B 123 (2019) 7599–7610.
[50] N. Sohrevardi, M.R. Bozorgmehr, M.M. Heravi, M. Khanpour, Transport properties of mixtures composed of iso-propanol, water, and supercritical carbon dioxide by molecular dynamics simulation, Bulgarian Chemical Communications 49 (2017) 92–98.
[51] M. Muñoz-Muñoz, G. Guevara-Carrion, J. Vrabec, Molecular insight into the liquid propan-2-ol + water mixture, J. Phys. Chem. B 122 (2018) 8718–8729.
[52] P.A. Artola, A. Raihane, C. Crauste-Thibierge, D. Merlet, M. Emo, C. Alba-Simionesco, B. Rousseau, Limit of Miscibility and Nanophase Separation in Associated Mixtures, J. Phys. Chem. B 117 (2013) 9718–9727.
[53] S. Banerjee, J. Furtado, B. Bagchi, Fluctuating micro-heterogeneity in water–tert-butyl alcohol mixtures and lambda-type divergence of the mean cluster size with phase transition-like multiple anomalies, J. Chem. Phys. 140 (2014) No. 194502.
[54] M.D. Hands, L.V. Slipchenko, Intermolecular Interactions in Complex Liquids: Effective Fragment Potential Investigation of Water−tert-Butanol Mixtures, J. Phys. Chem. B 116 (2012) 2775–2786.
[55] M. Kiselev, D. Ivlev, Y. Puhovski, T. Kerdcharoen, Preferential solvation and elasticity of the hydrogen bonds network in tertiary butyl alcohol–water mixture, Chemical Physics Letters 379 (2003) 581–587.
[56] I.A. Luk'yanchikova, D.V. Ivlev, M.G. Kiselev, G.A. Al'per, Concentration Dependence of the Viscosity of tert-Butanol - Water Mixtures: Physical Experiment and Computer Simulation, Russian Journal of General Chemistry 74 (8) (2004) 1156–1162.
[57] P.G. Kusalik, A.P. Lyubartsev, D.L. Bergman, A. Laaksonen, Computer Simulation Study of tert-Butyl Alcohol. 2. Structure in Aqueous Solution, J. Phys. Chem. B 104 (2000) 9533–9539.
[58] M.E. Lee, N.F. van der Vegt, A new force field for atomistic simulations of aqueous tertiary butanol solutions, J. Chem. Phys. 122 (2005) No. 114509.
[59] R. Gupta, G.N. Patey, Aggregation in dilute aqueous tert-butyl alcohol solutions: Insights from large-scale simulations, J. Chem. Phys. 137 (2012) No. 034509.
[60] S.D. Overduin, G.N. Patey, Comparison of simulation and experimental results for a model aqueous tert-butanol solution, J. Chem. Phys. 147 (2017) No. 024503.
[61] S. Paul, G.N. Patey, Why tert-Butyl Alcohol Associates in Aqueous Solution but Trimethylamine-N-oxide Does Not, J. Phys. Chem. B 110 (2006) 10514–10518.
[62] B. Kežić, A. Perera, Aqueous tert-butanol mixtures: A model for molecular-emulsions, J. Chem. Phys. 137 (2012) No. 014501.
[63] S.D. Overduin, A. Perera, G.N. Patey, Structural behavior of aqueous t-butanol solutions from large-scale molecular dynamics simulations, J. Chem. Phys. 150 (2019) No. 184504.
[64] M. di Pierro, M.L. Mugnai, R. Elber, Optimizing Potentials for a Liquid Mixture: A New Force Field for a tert-Butanol and Water Solution, J. Phys. Chem. B 119 (2015) 836–849.
[65] D.T. Bowron, J.L. Finney, A.K. Soper, Structural Investigation of Solute-Solute Interactions in Aqueous Solutions of Tertiary Butanol, J. Phys. Chem. B 102 (1998) 3551–3563.
[66] H. Tanaka, K. Nakanishi, Structure of aqueous solutions of amphiphilies: t-butyl alcohol and urea solutions, Fluid Phase Equilib 83 (1993) 77–84.

[67] D. González-Salgado, K. Zemánková, E.G. Noya, E. Lomba, Temperature of maximum density and excess thermodynamics of aqueous mixtures of methanol, J. Chem. Phys. 144 (2016) No. 184505.
[68] The William L. Jorgensen Research Group. http://zarbi.chem.yale.edu/
[69] M.A. González, J.L.F Abascal, A flexible model for water based on TIP4P/2005, J. Chem. Phys. 135 (2011) 224516.
[70] J.L.F. Abascal, C. Vega, A general purpose model for the condensed phases of water: TIP4P/2005, J. Chem. Phys. 123 (2005) No. 234505.
[71] D.V. der Spoel, E. Lindahl, B. Hess, G. Groenhof, A.E. Mark, H.J.C. Berendsen, GROMACS: fast, flexible, and free, J. Comput. Chem. 26 (2005) 1701–1718.
[72] S. Nosé, A molecular dynamics method for simulations in the canonical ensemble, Mol. Phys. 52 (1984) 255–268.
[73] W.G. Hoover, Canonical dynamics: Equilibrium phase-space distributions, Phys. Rev. A 31 (3) (1985) 1695–1697.
[74] M. Parrinello, A. Rahman, Polymorphic transitions in single crystals: A new molecular dynamics method, J. Appl. Phys. 52 (1981) 7182–7190.
[75] S. Nosé, M.L. Klein, Constant pressure molecular dynamics for molecular systems, Mol. Phys. 50 (1983) 1055–1076.
[76] U. Essmann, L. Perera, M.L. Berkowitz, T. Darden, H. Lee, L.G. Pedersen, A smooth particle mesh Ewald method, J. Chem. Phys. 103 (1995) No. 8577.
[77] G. Schaftenaar, CMBI, the Netherlands, MOLDEN a pre- and post processing program of molecular and electronic structure, http://cheminf.cmbi.ru.nl/molden/
[78] R.F. Lama, B.C.-Y. Lu, Excess Thermodynamic Properties of Aqueous Alcohol Solutions, J. Chem. Eng Data 10 (1965) 216–219.
[79] G.C. Benson, O. Kiyohara, Thermodynamics of Aqueous Mixtures of Nonelectrolytes. I. Excess Volumes of Water - n-Alcohol Mixtures at Several Temperatures, Journal of Solution Chemistry 9 (10) (1980) 791–804.
[80] M.I. Davis, E.S. Ham, Analysis and interpretation of excess molar properties of amphiphile + water systems Part 2. Comparisons of the propanol isomers in their aqueous mixtures, Thermochimica Acta 190 (1991) 251–258.
[81] Y. Koga, Excess partial molar enthalpies of water in water-tert-butanol mixtures, Can. J. Chem. 66 (1988) 3171–3175.
[82] Y. Koga, Differential heats of dilution of tert-butanol in water-tert-butanol mixtures at 26.90°C, Can. J. Chem. 64 (1986) 206–207.
[83] Y. Koga, Excess partial molar enthalpies of tert-butanol in water-tert-butanol mixtures, Can. J. Chem. 66 (1988) 1187–1193.
[84] P.K. Kpkemboi, A.J. Eastel, Densities and viscosities of binary aqueous mixtures of nonelectrolytes: tert-Butyl alcohol and tert-butylamine, Can. J. Chem. 72 (1994) 1937–1945.
[85] G.S. Kell, Density, ThermalExpansivity, and Compressibility of Liquid Water from 0° to 150°C: Correlations and Tables for Atmospheric Pressure and Saturation Reviewed and Expressed on 1968 Temperature Scale, J. Chem. Eng. Data 20 (1975) 97–105.
[86] D. González-Salgado, J. Troncoso, E. Lomba, The temperature of maximum density for amino acid aqueous solutions. An experimental and molecular dynamics study, Fluid Phase Equilibria 521 (2020) No. 112703.
[87] M.C. Despretz, Recherches sur le maximum de densitéde l'eau et des dissolitions aqueoses, Ann. Chim. Phys. 70 (1839) 49–81.